TJES

ISSN: 1813-162X

Tikrit Journal of Engineering Sciences

available online at: http://www.tj-es.com

Mass Transfer And Hydrodynamics In A Split-Column Airlift Photobioreactor

Amer D. Zmat

College of Engineering-University of Qadeseya, Qadeseya Province, Republic of Iraq

ABSTRACT

Overall gas-liquid mass transfer coefficients of oxygen gas (K_La) at different axial locations of the riser and downcomer of a split-column Airlift Photobioreactor were investigated using FOXY Fiber Optic oxygen sensor supported by NeoFox viewer software. The effect of bubble dynamics on mass transfer was considered. A 4-point optical probe was used to measure local interfacial area (a) and other bubble dynamics parameters for both the riser and the downcomer of a split-column airlift photobioreactor. Having both overall mass transfer (K_La) and interfacial area (a) measured at different locations, local oxygen mass transfer coefficient (K_L) can be determined for each location along the riser and the downcomer of the airlift bioreactor. Effects of different operating conditions (0.3 – 2.8 cm/s superficial gas velocity) on both mass transfer and bubble dynamics of the riser and the downcomer have been investigated for air-water system. It was found that both local mass transfer and gas-liquid interfacial area are considerably varying from the bottom to the top of the riser and the downcomer of the bioreactor. It was found that local mass transfer coefficient varies by 100% from the bottom to the top of the riser at low superficial gas velocity (1 cm/s) and by 30% at relatively high velocities (2-2.8 cm/s). The Trend of the variation of the K_La in the downcomer section of the column is very different from that of the riser, as it was noticed that insignificant mass transfer takes place at the lower part of the downcomer. The results of mass transfer and bubble dynamics in the riser and the downcomer of the studied conditions will be presented and discussed.

Keywords: Photo bioreactor, Airlift, Bubble dynamics, Optical fiber

INTRODUCTION

Airlift photo-bioreactors are basically a column divided into two parts, air/CO_2 is bubbled through only one side called the riser and other part is called the downcomer (Sanchez Miron et al., 2000). These bioreactors are extensively investigated for fermentation process and wastewater treatment (Znad et al. 2004, Znad et al. 2006) but have not been looked at as a replacement for the popular tubular photo-bioreactors until recent times (Sanchez Miron et al., 2000). The airlift photo-bioreactor is characterized by; high mass transfer, good mixing with low shear stress, low energy consumption, high potentials for scalability, easy to sterilize, good for immobilization of algae, reduced photo-inhibition.

However, the main limitations are; the small illumination surface area and decrease of illumination surface area upon scale-up. It has become clear that biological carbon sequestration and hydrogen production technologies have been poorly studied in the airlift photo-bioreactors and are in their infancy of development. PBRs can be classified into two types: open and closed systems (Pulz, 2001). Outdoor ponds are an example of open type PBR, but have the disadvantage of having no control over

process parameters and contamination caused by other microorganisms. Closed system overcomes these disadvantages by offering control over the process parameters. However, photobioreactor is far from being optimized. Hydrodynamics is a key parameter to determine the mass transfer of dissolved gases (O_2 and CO_2) in photobioreactors. Efficient mass transfer of CO_2 into the culture medium is desirable since un-dissolved CO_2 is lost by outgassing. Mass transfer of O_2 out of the system is also an important consideration, due to the need to remove photo-synthetically-derived O_2 before it reaches inhibitory concentrations. Gases introduced into bioreactors serve a number of purposes in microalgae cultivation, including: supply of CO_2 as sources of carbon for biomass metabolism; provision of internal mixing, which avoids nutrient concentration gradients, and stripping of accumulated dissolved oxygen, hence reducing its toxicity to microalgae ((Kumar et al., 2010, Pulz, 2001). Among the various alternatives, bubbling CO_2-enriched air into the bottom of the bioreactor with bubble diffusers has been the most frequently used approach. Moderate overall transfer efficiencies (13–20%) can be achieved by this mode of gas delivery (Carvalho et al. 2006); however, associated drawbacks are loss of CO_2 to the atmosphere, bio-fouling of diffusers, and poor mass transfer rates owing to a relatively low interfacial specific surface area. Relatively few researchers have quantified mass transfer coefficients in algal cultivation systems. Weismann et al. (1988) measured mass transfer coefficients for CO_2 from open ponds (100 m^2, 20 cm depth) and found K_La values of 0.2 and 0.5 h^{-1} for liquid velocities of 15 and 30 cm s^{-1}, respectively. Livansky (1990) reported mass transfer coefficients corresponding to K_La values of 5 to 8 h^{-1} at 20 °C for CO_2 from thin-layer open pond algae cultivation systems (50 m^2, 40–50 mm depth).

Oxygen transfer rate is described by the equation (Oosterhuis and Kossen, 1984):

$$\text{Oxygen transfer rate} = \frac{dC}{dt} = K_La\,(C^*-C) \quad \text{.....(1)}$$

Where (K_L) is the volumetric liquid phase mass transfer coefficient, (a) is the gas-liquid interfacial area available for mass transfer, (C*) is the oxygen concentration in the liquid at saturation, and (C) is the actual oxygen concentration in the liquid. Integrating equation (1) between the limits $C=C_0$ at t = 0 and C=C at t = t yields:

$$\ln\frac{C^*-C_0}{C^*-C} = K_L a t \quad \text{.....(2)}$$

The most well-known method to determine K_La is the unsteady-state method (Banerjee, 1993). A reactor is first filled with water, and then sparged with nitrogen to drive the oxygen out of the system (Shuler and Kargi, 2002). The air is then turned on and the changing oxygen concentration is recorded. Manipulating Equation 1 and graphing the results yields a straight line with a slope of negative K_La. This method is beneficial because it is simple, there are no chemicals required, and it can be applied to many different media types (Galaction *et al*., 2004). Mass transfer performance of airlift bioreactors has frequently stated in terms of an overall volumetric mass transfer coefficient K_La due to the difficulty of measuring true mass transfer coefficient K_L or local interfacial area (a). Recently, Sardeing, & Painmanakul, 2006 suggested the following equations to estimate specific interfacial area (a).

$$a = f_B\frac{H_L}{U_B}\frac{S_B}{V_{Total}} = \frac{N_{OR}xq}{V_B}\frac{H_L}{U_B}\frac{\pi d_B^2}{AH_L+N_BV_B} \quad \text{----------(3)}$$

$$a = \frac{6\varepsilon}{d_B(1-\varepsilon)} \quad \text{---------- (4)}$$

Despite the good agreement that they obtained between the predicted and measured values of interfacial area, their correlations depend on unpredictable parameters like f_B, d_B and N_B which may lead to probable discrepancy or make it difficult to predict the local values of interfacial area. Hence, the objective of

this paper is to use a Foxy optical probe from Ocean Optics and a sophisticated 4-point optical probe for measuring local oxygen concentration in liquid phase and hydrodynamics parameters (ε and a) at different locations of a split-column airlift bioreactor, to account for the effect of the variation of the interfacial area on the mass transfer coefficient of air-water system.

EXPERIMENTS

1.Experimental set-up

The split-column airlift reactor and the flow scheme used in this study are shown schematically in Figure (1) which is similar to that of Luo and Al-Dahhan (2005) in order to have this study findings and results comparable to those of Luo and Al-Dahhan (2005). The column was made from Plexiglas with an inner diameter of 13 cm and height of 150 cm. A Plexiglas plate divides the reactor into two zones of equal cross-sectional areas. The liquid volume of the reactor is 15 liters. The top clearance (the distance from the top edge of the splitting plate to the static liquid level) was 3 cm while the bottom clearance was 5 cm. At the bottom of the riser section of the reactor, a sparger (Fig.1-b) was installed at the center of the riser. The column has 5 ports (P1 through P5 in the figure) on both sides (riser and downcomer) for hydrodynamics and oxygen concentrations measurements. These ports are at heights of 29,90cm, 52.00 cm, 76.05cm, and 100.1 cm (equivalent to 4.6R, 8R, 11.7R, 15.4R) respectively. The set-up was operated in a batch mode with deionized water as the liquid phase. The column was run at different operating conditions (superficial gas velocity ranges from 0.3 cm/s to 2.8 cm/s). A four-point optical probe (shown in Fig.3) was employed to investigate the bubble dynamics in the riser and downcomer of the split-column airlift bioreactor. The optical probe was positioned downwards in the riser to ensure it faces the upward moving bubbles, while it was pointed upwards in

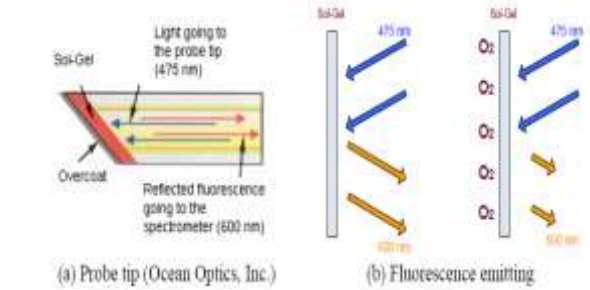

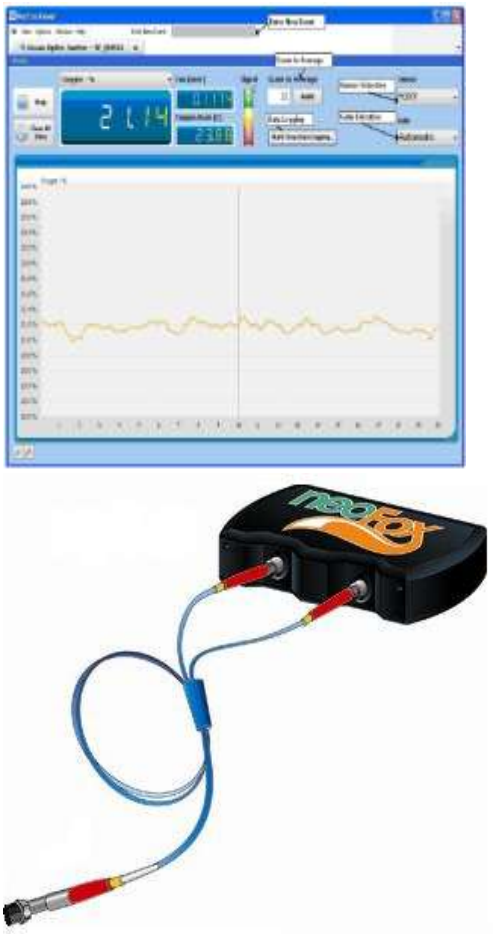

(c) NeoFox viewer screen

(d) NeoFox kit

Fig.2 Foxy probe for Oxygen Concentration measurements

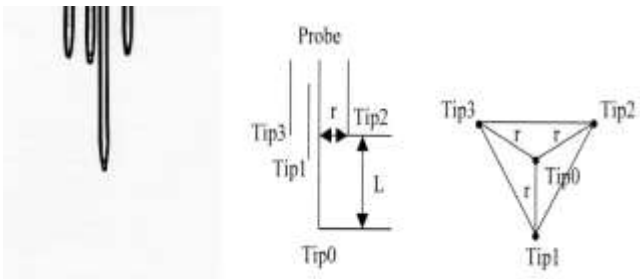

Fig.3 4- Point optical probe

the downcomer so that it faces the downwards moving bubbles. The optical probe was used to measure the hydrodynamic performance of both the riser and the downcomer at different positions through the provided ports. A data processing algorithm developed by Xue (2004) was used, with which local gas hold-up and specific interfacial area was measured.

2.Procedure

The split-column airlift bioreactor was operated in batch mode with (15) liters distilled water hold-up. Before experiments were carried out, oxygen probe was calibrated using two-point calibration method which is described elsewhere (NeoFox installation and operation manual). Two-point calibration is based on two known concentrations, one being the 0% oxygen concentration. Nitrogen was sparged for at least (20) minutes to strip dissolved oxygen from water and degassed it out of the reactor to obtain 0% oxygen concentration. Then oxygen probe was exposed to the 0% oxygen concentration to record the first point of calibration. To determine the second point of calibration, the column was emptied from water and the probe was exposed to ambient conditions in air which is 20.9% oxygen and represents the second point of calibration. Hence, both oxygen and optical probes were used for oxygen concentration and bubble dynamics measurements at different locations of the column for the following superficial gas velocities (U_g = 0.3, 1, 2, 2.8 cm/s).

RESULTS and DISCUSSION

Local mass transfer coefficient of oxygen in the riser section of the column

The K_La of oxygen at different locations of the column (4.6R, 8R, 11.7R and 15.4R from the bottom of the column at the center of the riser section, R: 6.5) are shown in Fig.(4). The K_La profiles at different superficial gas velocities clearly show different trends of variation. At low

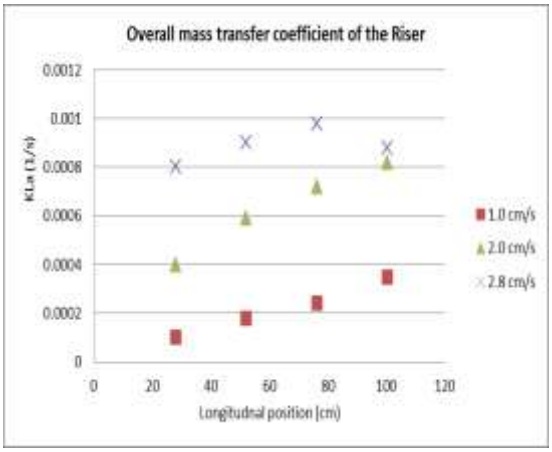

Fig.4 Overall mass transfer coefficient profiles of the riser section of a split-column airlift bioreactor at different superficial gas velocities.

velocity (0.3 cm/s), the obtained data were scattered and unreliable, so it was ignored. At superficial gas velocity of 1 cm/s, the K_La showed 100% increase from the bottom to the top of the riser section of the column. For higher gas velocities (2, 2.8 cm/s), the rate of increase of the K_La from the bottom to the top of the column was 30% and 22.5% respectively. It was also noticed that the rate of change of K_La at the upper middle of the column tends to decline by 11% at the top of the column. This is attributed to the degassing phenomena that take place at the top surface of the liquid (i.e. rapid disengagement of bubbles from the liquid phase). The profiles of the specific interfacial area of the riser section of the column at different gas velocities are shown in Fig.(5).

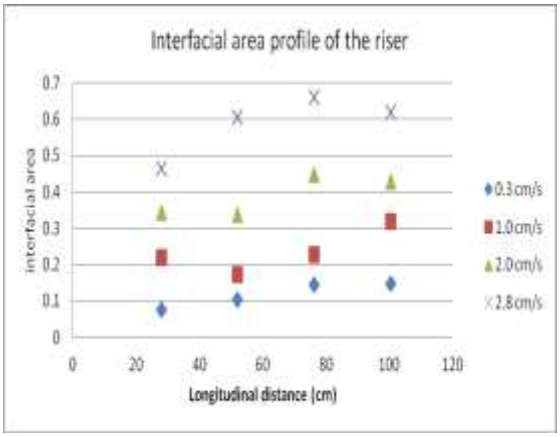

Fig.5 Interfacial area profiles of the riser section of a split-column airlift bioreactor at different superficial gas velocities.

At low velocity (0.3), the interfacial area showed 58% increase from the bottom to the top due to low interaction of bubbles and non-coalescence nature of water. When superficial gas velocity increased to 1 cm/s, 21% decrease in interfacial area was developed at the lower middle of the column, due to the interaction of the swarm of the bubbles after leaving the sparger. At higher velocities, the upper middle of the column witnessed 9% decrease in the value of the interfacial area. This is attributed to the rapid disengagement of the bubbles from the top surface of the liquid. Having obtained both the ($K_L a$) and oxygen local mass transfer coefficient was determined using the below equation:

$$K_L = \frac{K_L a}{a} \quad \text{..... (5)}$$

Fig.(6) shows how K_L varies from the bottom to the top of the column. The effect of the superficial gas velocity on the K_L is also shown. At gas velocities of 0.3 and 1 cm/s, the local mass transfer of oxygen shows 69% increase in the lower middle of the column, then a decrease of 61% was noticed in the upper middle of the column. It is easily concluded that the middle of the riser section of the column will be the higher mass transfer coefficient.

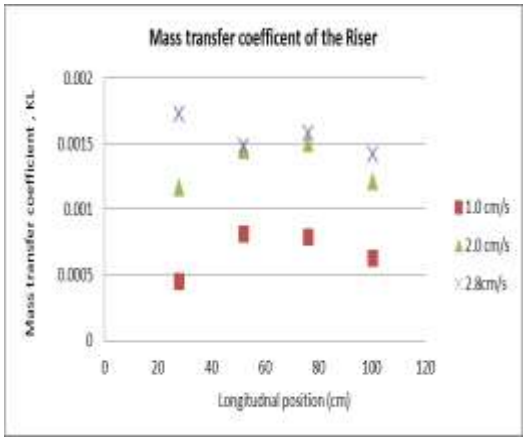

Fig.6 Local mass transfer coefficient variation with longitudinal position of the riser at different values of superficial gas velocities.

Procedure

The split-column airlift bioreactor was operated in batch mode with (15) liters distilled water hold-up. Before experiments were carried out, oxygen probe was calibrated using two-point calibration method which is described elsewhere (NeoFox installation and operation manual). Two-point calibration is based on two known concentrations, one being the 0% oxygen concentration. Nitrogen was sparged for at least (20) minutes to strip dissolved oxygen from water and degassed it out of the reactor to obtain 0% oxygen concentration. Then oxygen probe was exposed to the 0% oxygen concentration to record the first point of calibration. To determine the second point of calibration, the column was emptied from water and the probe was exposed to ambient conditions in air which is 20.9% oxygen and represents the second point of calibration. Hence, both oxygen and optical probes were used for oxygen concentration and bubble dynamics measurements at different locations of the column for the following superficial gas velocities (U_g = 0.3, 1, 2, 2.8 cm/s).

RESULTS AND DISCUSSIONS

Local mass transfer coefficient of oxygen in the riser section of the column

The $K_L a$ of oxygen at different locations of the column (4.6R, 8R, 11.7R and 15.4R from the bottom of the column at the center of the riser section, R: 6.5) are shown in Fig.(4). The $K_L a$ profiles at different superficial gas velocities clearly show different trends of variation. At low velocity (0.3 cm/s), the obtained data were scattered and unreliable, so it was ignored. At superficial gas velocity of 1 cm/s, the $K_L a$ showed 100% increase from the bottom to the top of the riser section of the column. For higher gas velocities (2, 2.8 cm/s), the rate of increase of the $K_L a$ from the bottom to the top of the column was 30% and 22.5% respectively. It was also noticed that the rate of change of $K_L a$ at the upper middle of the column tends to decline by 11% at the top of the column. This is attributed to the degassing phenomena that take place at the top surface of the liquid (i.e. rapid disengagement of bubbles from the liquid

phase). The profiles of the specific interfacial area of the riser section of the column at different gas velocities are shown in figure (5). At low velocity (0.3), the interfacial area showed 58% increase from the bottom to the top due to low interaction of bubbles and non-coalescence nature of water. When superficial gas velocity increased to 1 cm/s, 21% decrease in interfacial area was developed at the lower middle of the column, due to the interaction of the swarm of the bubbles after leaving the sparger. At higher velocities, the upper middle of the column witnessed 9% decrease in the value of the interfacial area. This is attributed to the rapid disengagement of the bubbles from the top surface of the liquid. Having obtained both the (K_La) and oxygen local mass transfer coefficient was determined using the below equation:

$$K_L = \frac{K_L a}{a} \quad \text{.....(5)}$$

Fig.(6) shows how K_L varies from the bottom to the top of the column. The effect of the superficial gas velocity on the K_L is also shown. At gas velocities of 0.3 and 1 cm/s, the local mass transfer of oxygen shows 69% increase in the lower middle of the column, then a decrease of 61% was noticed in the upper middle of the column. It is easily concluded that the middle of the riser section of the column will be the higher mass transfer coefficient.

2.Local mass transfer coefficient of oxygen in the downcomer section of the column

Fig.(7) shows demonstrates the overall mass transfer coefficient K_La of downcomer section of the column under the same superficial gas velocities of the riser. At 0.3 cm/s gas velocity, no data were obtained. At 1 cm/s gas velocity, it was noticed that the overall mass transfer coefficient stays almost constant at 4.6R, 8R, 11.7R positions, and 100% increase was developed at the top of the downcomer section of the column. This

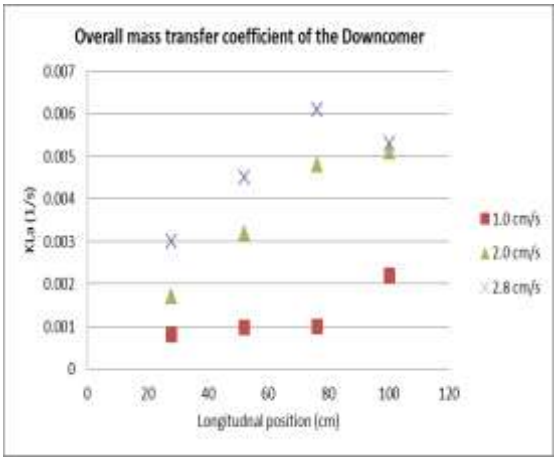

Fig.7 Overall mass transfer coefficient profiles of the downcomer section of a split-column airlift bioreactor at different superficial gas velocities.

significant increase is attributed to the high mixing which happens at the top of the column and relatively long time of residence of bubbles due to turbulence and buoyant bubbles. At relatively higher velocities (2-2.8 cm/s), the K_La increases by 170% from the bottom to the top of the downcomer. At superficial gas velocity of 2.8 cm/s, the K_La witnesses 17% decrease from 11.7R to 15.4R positions. These is due to the rapid disengagement of bubbles at the surface of the liquid, while the high mixing and bubbles interactions that take place at the position 1.7R results in higher residence time of bubbles and accordingly higher mass transfer. Fig.(8) shows the trend of change of the specific interfacial area of the downcomer from the bottom to the top. Detailed discussions of these phenomena are shown elsewhere (Albdiri, Amer et al, TBP).

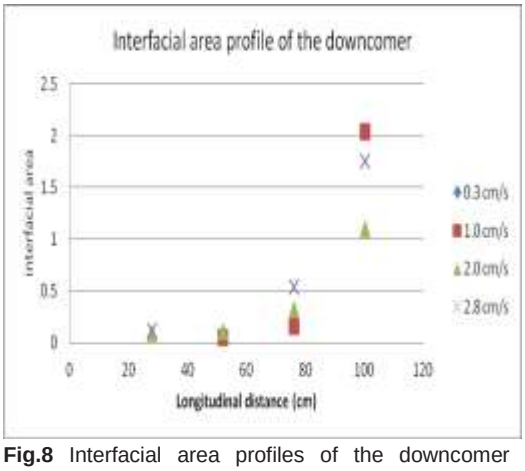

Fig.8 Interfacial area profiles of the downcomer section of a split-column airlift bioreactor at different superficial gas velocities.

Fig.(9) clearly shows that insignificant mass transfer occurs at the bottom of the downcomer for all gas velocities and only the upper part of the downcomer witness considerable mass transfer.

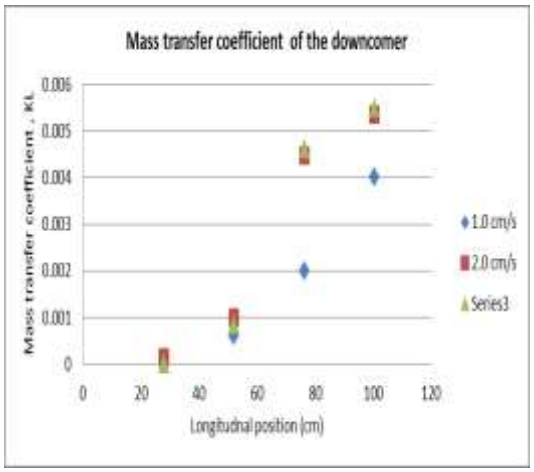

Fig.9 Local mass transfer coefficient variation with longitudinal position of the downcomer at different values of superficial gas velocities.

CONCLUSIONS

Local mass transfer coefficients and local bubble dynamics measurements at different axial locations were carried out using FOXY probe from Ocean Optic inc and 4-point optical probe (in-house made) respectively. The FOXY probe is a chemical-sensing device with fluorescing properties, integrated to spectrometer and PC interface. It directly measures the oxygen concentration. K_La is determined from the unsteady-state conditions (between 10% to 80% saturated oxygen concentrations) according to the well-known method (Oosterhuis and Kossen, 1984). The K_La of the riser is different from that of the downcomer due to the difference in the hydrodynamics characteristics of the riser from that of the downcomer. At low superficial gas velocities (1 cm/s), both the riser and the downcomer exhibit linear and small increase of K_La from the bottom to the top of the column. At relatively high gas velocities (2, 2.8 cm/s), K_La shows less rate of increase from the bottom to the top of the column (both riser and downcomer). The 4-point optical probe efficiently measures local interfacial area for both riser and downcomer. These measurements and FOXY probe measurements allow us to determine local mass transfer for both the riser and the downcomer of the column. The local mass transfer coefficients of the riser are significantly different from those of the downcomer; moreover, the lower part of the downcomer does not witness considerable mass transfer due to the absence of gas bubbles. Therefore, most of the mass transfer process will be carried out in the riser section of the column and the upper part of the downcomer of the airlift bioreactors. Mapping the oxygen mass transfer inside a split-column photobioreactor is very essential to envision the microalgae growth environment and the O_2-CO_2 exchange rate that assure the consumption of nutrients (CO_2) and the removal of the photo-synthetic oxygen before it becomes inhibitory material for algae growth.

ACKNOWLEDGEMENT

The author would like to acknowledge the support of Prof. Muthanna Al-Dahhan, Chairman of the chemical and biochemical Engineering Department, Missouri University of Science and Technology during this course of research which was accomplished at Al-Dahhan Labs. Also, the financial support of the CRDF Global is greatly appreciated.

REFERENCES

1- Sanchez Miro´n, A., Garcia Camacho, F., Contreras Gomez, A., Molina Grima, E. and Chisti, Y., 2000, Bubble column and airlift photobioreactors for algal culture, AIChE J, 46: 1872–1887.

2- Hussein Znad, Gita Naderi, H.M. Ang and M.O. Tade, " CO2 Biomitigation and Biofuel Production Using Microalgae: Photobioreactors Developments and Future Directions", Curtain University, Australia, 2004.

3- NeoFox installation and operation manual, document number: 013-20000-009-02-201008.

4- O. Pulz, photobioreactors: production systems for phototrophic microorganisms, Appl. Microbial Biotechnology (2001), 57:287-293.

5- Matam Vijay-Kumar, Jesse D. Aitken, Fredric A. Carvalho, Tyler C. Cullendor, Simon Mwangi, 'Metabolic Syndrome and Altered Gut Microbiota in Mice lacking Toll-Like receptor 5, Science 2010.
6- Carvalho, A.P. et al. (2006) Microalgal reactors: a review of enclosed systems design and performances. Biotechnol. Prog. 22, 1490–1506.
7- Livansky K. 1990. Losses of CO_2 in outdoor mass cultures: Determination of the mass transfer coefficient KL by means of the measured pH course in NaHCO3 solution. Algological Studies, 58: 87–97.
8- Weissman J.C., Goebel R.P. and Benemann J.R. 1988. Photobioreactor design: Mixing, carbon utilization, and oxygen accumulation. Biotechnol. Bioeng. 31: 336–344.
9- Banerjee UC. 1993. Effect of stirrer speed, aeration rate, and cell mass concentration on volumetric oxygen transfer coefficients (kLa) in the cultivation of *Curvularia lunata* in a batch reactor. Biotechnol Tech 7:733-738.
10- Shuler ML, Kargi F. 2002. Bioprocess engineering. Upper Saddle River, New Jersey: Prentice Hall.
11- Galaction, A.I., D. Cascaval, C. Oniscu and M. Turnea, 2004. Enhancement of oxygen mass transfer in stirred bioreactors using oxygen vectors. 1. Simulated fermentation broths. Bioprocess Biosyst. Eng., 26: 231-238.
12- Rudolph Sardeing, Pisut Painmanakul, Gilles Hébrard (2006). Effect of surfactants on liquid-side mass transfer coefficients in gas–liquid systems: first step to modeling, Chemical Engineering Science 61, 6249 – 6260
13- Hu-Ping Luo, M. H. Al-Dahhan, (2005). Analyzing and Modeling of Airlift Photobioreactors for Microalgal and Cyanobacteria Cultures, D. Sc. Dissertation, Washington University Saint Louis, Missouri.
14- Junli Xue, Muthanna Al-Dahhan, M. P. Dudukovic1 and R. F. Mudde, Bubble Dynamics Measurements Using Four-Point Optical Probe, The Canadian Journal of Chemical Engineering, Volume 81, June-August 2003.

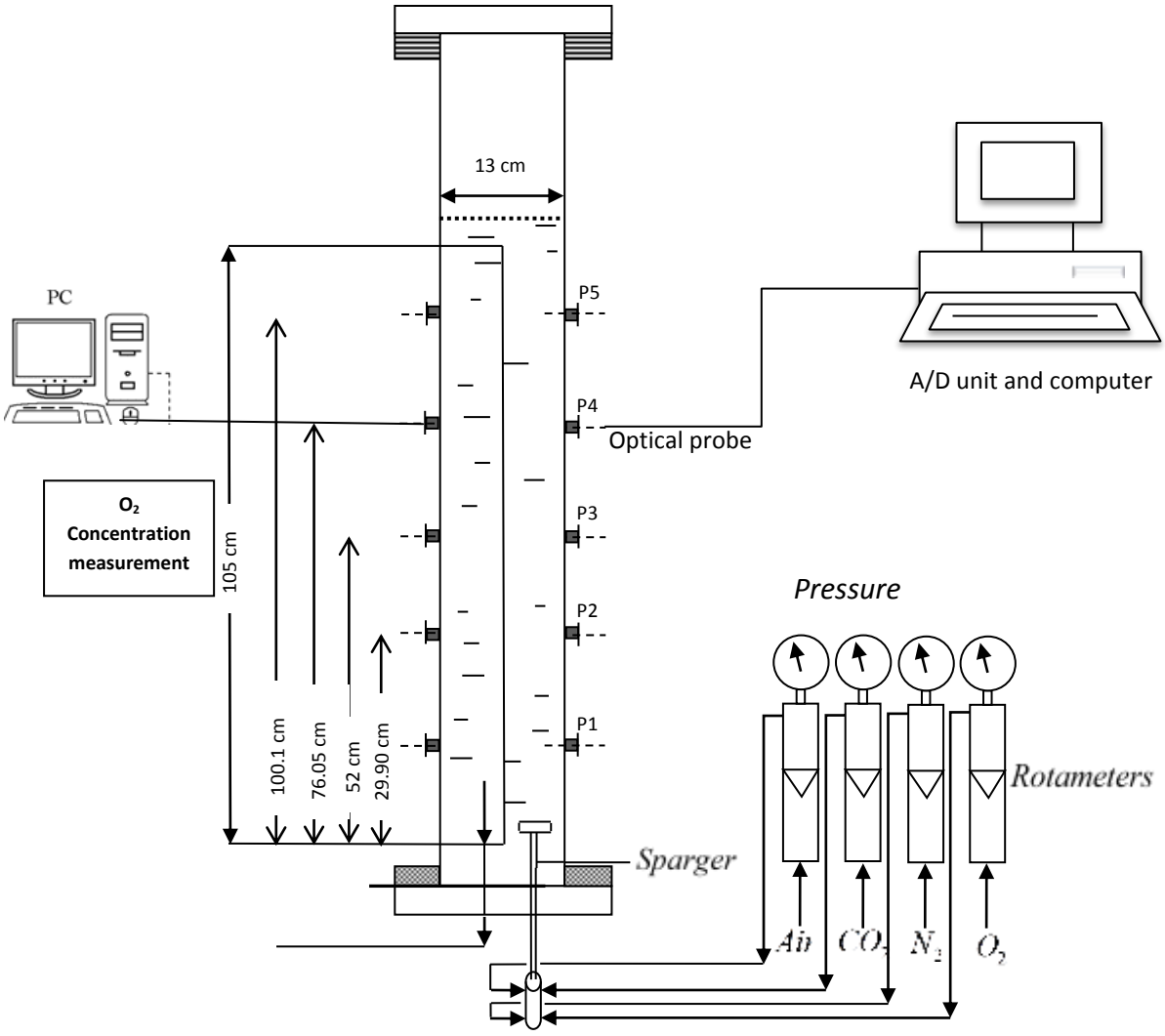

Fig.1-a Split-column; oxygen and optical probes are connected.

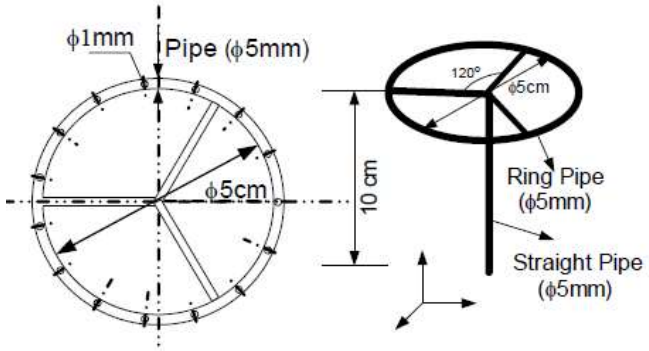

Fig.1-b Sparger

Fig.1 Schematic representation of split-column airlift bioreactor and sparger.